IOPscience iopscience.iop.org

Home Search Collections Journals About Contact us My IOPscience

Electronic states of a semi-infinite superlattice with an embedded quantum well

This article has been downloaded from IOPscience. Please scroll down to see the full text article.

1995 J. Phys.: Condens. Matter 7 3493

(http://iopscience.iop.org/0953-8984/7/18/013)

View the table of contents for this issue, or go to the journal homepage for more

Download details:
IP Address: 171.66.16.179
The article was downloaded on 13/05/2010 at 13:04

Please note that terms and conditions apply.

J. Phys.: Condens. Matter 7 (1995) 3493–3500. Printed in the UK

Electronic states of a semi-infinite superlattice with an embedded quantum well

J Arriaga† and V R Velasco‡

† Instituto de Física 'Luis Rivera Terrazas', Benemérita Universidad Autónoma de Puebla, Apartado Postal J-48, Puebla, Pue 72750, Mexico

‡ Instituto de Ciencia de Materiales, Consejo Superior de Investigaciones Científicas, Serrano 123, 28006 Madrid, Spain

Received 24 October 1994, in final form 22 March 1995

Abstract. We study the electronic states at the $\bar{\Gamma}$ point of a heterostructure, formed by a semi-infinite substrate (AlAs), a well material (GaAs) and a semi-infinite superlattice (AlAs/GaAs), grown along the [001] direction. We employ an empirical tight binding (ETB) Hamiltonian together with the surface Green function matching (SGFM) method. We study the effect of the well layer width and the relative thicknesses of the layers forming the superlattice on the energy values and spatial localization of the different states (near the main gap at the $\bar{\Gamma}$ point) of this heterostructure.

1. Introduction

When a superlattice is grown on a substrate it is possible to have Tamm-like states at the end of the semi-infinite superlattice terminating in a well slab followed by the substrate, which acts as a thick barrier. In recent years there has been a growing interest in the study of the interface between a superlattice and the substrate. Tamm states have been observed experimentally [1, 2] by means of a combination of photoluminescence, photoluminescence excitation and photocurrent spectroscopies. Also interface quantum well states have been observed by three-wave-mixing spectroscopy in ZnSe/GaAs heterostructures [3]. Embedded quantum wells have recently been studied experimentally [4, 5]. Theoretical calculations of these states have been performed within the framework of the Kronig–Penney model [6]. Semi-infinite superlattices have been studied by using the Kronig–Penney model [7, 8, 9, 10], a two-band tight-binding model [11] and a tight-binding envelope scheme [12, 13]. Quite recently, and as a first step to attack the embedded quantum well in a semi-infinite superlattice, we studied the ideal semi-infinite superlattice by means of an elaborate ETB Hamiltonian, which gives a good description of the electronic properties of bulk semiconductors and infinite superlattices, together with the surface Green function matching (SGFM) method [14]. We studied in this way (001) AlAs/GaAs superlattices [15] and strained (001) GaAs/GaP superlattices [16]. In both cases we studied the influence of the position of the terminating layer on the energy levels and spatial penetration of the surface states. The formal and numerical aspects of those studies will be used now to consider the heterostructures grown along the [001] direction and formed by a semi-infinite substrate (AlAs), a well layer (GaAs) and a semi-infinite superlattice (AlAs/GaAs). We shall study the influence of the width of the well layer and the relative thicknesses of the materials forming the superlattice on the energy values and real space localization of the

0953-8984/95/183493+08$19.50 © 1995 IOP Publishing Ltd

electronic states of the system. We shall concentrate on the lowest conduction band (CB) and highest valence band (VB) states and we shall compare also the situation with the infinite superlattice case.

In section 2 we discuss briefly the theoretical framework and some formal aspects of the calculations. In section 3 we present the results of our calculations for different superlattice periods combined with different values of the width of the well layer. Conclusions are presented in section 4.

2. Theoretical basis

Our calculations have been performed with an ETB Hamiltonian with a sp^3s^* orbital basis [17], including spin–orbit splitting [18], and interactions up to nearest neighbours only, using the SGFM method. For the semi-infinite superlattice the geometry, notation, size of the matrices and numerical algorithms to calculate the Green functions are the same as those previously employed for the infinite superlattices [19].

We shall continue to use the concept of a *principal layer* which is defined so that each one interacts only with nearest-neighbour principal layers and this accounts for all interactions in the crystal. With the model employed here a principal layer consists of two atomic layers, one of anions and one of cations.

We recall some basic formal considerations concerning the case of the semi-infinite superlattice. The Green function one obtains for the infinite superlattice [19], which we shall denote by G_{SL}, depends on κ (the wavevector parallel to the interfaces), E (energy), n, n' (layer indices) and q (the 1D wavevector associated with the superperiodicity of the superlattice). This means that $G_{\mathrm{SL}}(n, n'; q)$ is the *structural Green function* of the superlattice and thus q must be eliminated in order to study the semi-infinite superlattice [15, 16] which no longer has supertranslation symmetry. It has been shown [20] that the correct Green function needed to study the semi-infinite superlattice is

$$G_{\bar{\mathrm{SL}}}(\kappa, n, n') = \frac{1}{2\pi L} \int_{-\pi}^{\pi} G_{\mathrm{SL}}(\kappa, n, n'; qL)\, \mathrm{d}(qL) \tag{1}$$

L being the period of the superlattice. This Green function can then be used to study the semi-infinite superlattice [15, 16] in the same way as the ordinary Green function of a crystal is employed to study the semi-infinite crystal.

As in the usual symmetric (001) quantum well with a structure of type B–A–B [14, 21], the manner in which a given atom in the interface layers is bonded to the others is the same for the ℓ (left) and r (right) interfaces. Thus we shall employ, for the parameters of the As atoms at ℓ and r interfaces, the arithmetic mean of the bulk GaAs and AlAs parameters. However, in the present case we have a semi-infinite AlAs–GaAs well–semi-infinite AlAs/GaAs superlattice, which is an asymmetric quantum well structure of B–A–C type. Therefore we must modify accordingly some of the formal expressions of the symmetric well. We note, incidentally, that we have not performed a self-consistent tight-binding calculation [22, 23] because this would be very costly in computer time while not modifying significantly the overall picture emerging from the calculations. We now give the essential expressions needed for the calculation.

The projection at the interfaces of the system Green function is given by

$$\tilde{G}_{\mathrm{s,A}}^{-1} = \begin{bmatrix} \ell_{\mathrm{B}}(E-H_{\mathrm{s}})\ell_{\mathrm{B}}-\ell_{\mathrm{B}}D_{\mathrm{B}}\ell_{\mathrm{B}} & -\ell_{\mathrm{B}}H_{\mathrm{l}}\ell_{\mathrm{A}} & 0 & 0 \\ -\ell_{\mathrm{A}}H_{\mathrm{l}}\ell_{\mathrm{B}} & \ell_{\mathrm{A}}(E-H_{\mathrm{s}})\ell_{\mathrm{A}}-\ell_{\mathrm{A}}D_{\mathrm{A}}\ell_{\mathrm{A}} & -\ell_{\mathrm{A}}D_{\mathrm{A}}r_{\mathrm{A}} & 0 \\ 0 & -r_{\mathrm{A}}D_{\mathrm{A}}\ell_{\mathrm{A}} & r_{\mathrm{A}}(E-H_{\mathrm{s}})r_{\mathrm{A}}-r_{\mathrm{A}}D_{\mathrm{A}}r_{\mathrm{A}} & -r_{\mathrm{A}}H_{\mathrm{l}}r_{\mathrm{C}} \\ 0 & 0 & -r_{\mathrm{C}}H_{\mathrm{l}}r_{\mathrm{A}} & r_{\mathrm{C}}(E-H_{\mathrm{s}})r_{\mathrm{C}}-r_{\mathrm{C}}D_{\mathrm{C}}r_{\mathrm{C}} \end{bmatrix} \tag{2}$$

The notation is as in the usual SGFM calculations [14, 21]: ℓ_B denotes the B part of the ℓ interface B–A, r_A the A part of the r interface A–C and so on. All the expressions for the A part are the same as those given in [21]. On the other hand, for the parts with subindexes B and C we have

$$\begin{bmatrix} H_B(2,1) & 0 \\ 0 & H_B(1,2) \end{bmatrix} \begin{bmatrix} \bar{T}_B & 0 \\ 0 & G_{\bar{S}L}(2,1) \end{bmatrix} = \begin{bmatrix} \ell_B D_B \ell_B & 0 \\ 0 & r_C D_C r_C \end{bmatrix}. \tag{3}$$

Taking ℓ_B as the origin, we have for layer n_B to the left of the ℓ interface (corresponding to AlAs)

$$G_s(n_B, n_B) = \mathcal{G}_B + \left[\bar{T}_B^{(n_B+1)}, 0\right] \mu_B \begin{bmatrix} \bar{S}_B^{(n_B+1)} \\ 0 \end{bmatrix} \tag{4}$$

where

$$\begin{aligned} \mu_B &= (\tilde{G}_{s,A} - \tilde{g}_B \sigma_B) \\ \tilde{g}_B &= \begin{bmatrix} \mathcal{G}_B & 0 \\ 0 & 0 \end{bmatrix} \\ \mathcal{G}_B &= G_B(n_B, n_B) \end{aligned} \tag{5}$$

and for layer n_C to the right of interface r

$$G_s(n_C, n_C) = \mathcal{G}_C + \left[0, G_{\bar{S}L}(n_C, \nu_A + 2)\right] \mu_C \begin{bmatrix} 0 \\ G_{\bar{S}L}(\nu_A + 2, n_C) \end{bmatrix} \tag{6}$$

where

$$\begin{aligned} \mu_C &= \begin{bmatrix} 0 & 0 \\ 0 & \mathcal{G}_C^{-1} \end{bmatrix} (\tilde{G}_{s,A} - \tilde{g}_C \sigma_C) \begin{bmatrix} 0 & 0 \\ 0 & \mathcal{G}_C^{-1} \end{bmatrix} \\ \tilde{g}_C &= \begin{bmatrix} 0 & 0 \\ 0 & \mathcal{G}_C \end{bmatrix} \\ \mathcal{G}_C &= G_{\bar{S}L}(\nu_A + 2, \nu_A + 2). \end{aligned} \tag{7}$$

The above demonstrate the differences between the case treated here and that of the quantum well of type B–A–B, described elsewhere [14, 21].

3. Results and discussion

We have calculated the electronic states at the $\bar{\Gamma}$ point, $\kappa = (0, 0)$, of (001) heterostructures. We have used the following energy reference $E_V(\text{AlAs}) = 0$ eV, $E_C(\text{AlAs}) = 2.30$ eV, which corresponds to the AlAs indirect band gap, $E_V(\text{GaAs}) = 0.55$ eV and $E_C(\text{GaAs}) = 2.10$ eV. This band offset is within experimentally accepted values for (001) interfaces. We have considered here the results of the self-consistent tight-binding calculations on the formation of heterojunctions [24, 25, 26], which show that a semiconductor interface is basically formed with two monolayers of a second semiconductor deposited on a semiconductor substrate. The empirical tight-binding parameters employed in our calculations are the same as those in [21]. They take into account the spin–orbit coupling and thus they are different from those of [17]. This parametrization gives effective masses for the conduction electrons at the Γ point of $m^* = 0.106$ for GaAs and $m^* = 0.249$ for AlAs, which are higher than those experimentally measured, $m^* = 0.065$ for GaAs and $m^* = 0.19$ for AlAs. In spite of this fact this parametrization has given good results when compared with experimental data in the case of (311) AlAs/GaAs superlattices [27, 28], and triangular [29] and inverse parabolic quantum wells [30]. It could be possible to improve the effective

masses of the conduction electrons by using a Hamiltonian including interactions up to second neighbours. We would then have more parameters at our disposal and it could then be possible to improve the results obtained with the simpler Hamiltonian. Another possibility would be to use different parametrization schemes to fit the effective masses [31, 32]. This would not modify the overall picture emerging from the calculations, but some details concerning the thicknesses of the layers where the different localizations appear, and the numerical values of the different energy levels would be affected, as can be seen when comparing the results of [27, 28] with those of [31]. Because of these reasons we decided to stay with the simpler parametrization in order to obtain the general physical picture.

We have performed calculations for different quantum wells embedded between a semi-infinite AlAs substrate, to the left, and three different semi-infinite superlattices, $(AlAs)_4/(GaAs)_4$, $(AlAs)_4/(GaAs)_{12}$ and $(AlAs)_{12}/(GaAs)_4$ respectively, to the right. The width of the GaAs layer in the well region ranges from 4 to 12 principal layers with an increase of 2 principal layers for every new quantum well considered. Our calculations are not self-consistent and this can raise some questions when the slabs considered are not very large, as in our case. A self-consistent tight-binding calculation for this problem would be quite costly in computer resources and it would not modify the general trends obtained here. We must consider that the tight-binding calculations have their main strength in providing these general trends for different thicknesses of the layers in a simple way. Even the numerical values are quite good in general, even for the crudest models. In fact we have seen that non-self-consistent calculations for superlattices with very thin layers, one or two monolayers wide, agree reasonably well with the experimental data available for those systems [33]. Thus one may reasonably expect that the general trends resulting from this type of calculation can be considered valid even if we are neglecting self-consistency for the tight-binding calculations.

We have checked the character of the different states found in our calculations by obtaining the distribution of spectral strength in the different layers of the embedded quantum wells and in four layers of the substrate to the left and one whole period of the superlattice to the right, respectively. We have restricted our study to the lowest states in the conduction band (CB) and the highest states in the valence band (VB). The results are summarized in table 1. In table 2 we present the same states for the three corresponding infinite superlattices. It can be seen from table 1 that for some thicknesses the states are not localized in the well layers, but in the superlattice. It can also be seen that in some cases there is localization in the embedded well and in the superlattice. In these cases it can be seen by looking at table 2 that the energies are quite close to those of the corresponding states in the infinite superlattices and the thickness of the layer is quite close to that of the GaAs layer in the superlattice. We find localized states in the embedded well region for thicknesses which depend on the superlattice period and the thicknesses are also different for the CB and VB states for a given superlattice. We can see that in the cases analysed we obtain CB bound states when $n \geqslant 8$, n being the number of GaAs layers in the embedded well, as in the normal quantum wells [21]. But the situation is different for the VB states. In this case we obtain bound states for some thicknesses only, as opposed to the normal quantum well case, in which there were always bound states for any quantum well thickness [21].

We present in figure 1 the distribution of the spectral strength of the states considered in table 1, in the different layers of the 4-layer quantum well embedded in the (4,4) superlattice. This also displays the localization of the different states. Figure 2 gives the same information for the 8-layer embedded quantum well.

Table 1. Energies, in eV, and localization (in parentheses) of the lowest CB state and the two highest VB states at the $\bar{\Gamma}$ point of embedded $(GaAs)_n$ quantum wells, $(4 \leqslant n \leqslant 12)$, between an AlAs substrate and three different AlAs/GaAs semi-infinite superlattices. (QW) denotes localization in the GaAs well region; (A) denotes localization in the AlAs layers of the superlattice and (B) denotes localization inside the GaAs layers of the superlattice.

N_{QW}	4	6	8	10	12
			$(AlAs)_4/(GaAs)_4$ SL		
CB1	2.32 (SL,A)	2.32 (SL,A)	2.27 (QW)	2.24 (QW)	2.21 (QW)
VB1	0.39 (SL,B)	0.40 (QW;SL,B)	0.45 (QW)	0.48 (QW)	0.49 (QW)
VB2	0.30 (QW)	0.31 (QW)	0.38 (QW;SL,B)	0.41 (QW;SL,B)	0.44 (QW)
			$(AlAs)_4/(GaAs)_{12}$ SL		
CB1	2.23 (SL,B)	2.22 (SL,B)	2.22 (SL,B)	2.22 (QW;SL,B)	2.21 (QW,SL,B)
VB1	0.51 (SL,B)	0.51 (SL,B)	0.51 (SL,B)	0.51 (QW)	0.51 (QW;SL,B)
VB2	0.46 (SL,B)	0.47 (SL,B)	0.47 (QW;SL,B)	0.48 (QW;SL,B)	0.49 (QW;SL,B)
			$(AlAs)_{12}/(GaAs)_4$ SL		
CB1	2.28 (SL,A)	2.28 (SL,A)	2.27 (QW;SL,A)	2.24 (QW)	2.21 (QW)
VB1	0.39 (SL,B)	0.39 (QW;SL,B)	0.45 (QW)	0.48 (QW)	0.49 (QW)
VB2	0.30 (QW;SL,B)	0.31 (QW;SL,B)	0.38 (SL,B)	0.41 (QW)	0.44 (QW)

Table 2. Energies in eV, and localization (in parentheses) of the lowest CB state and the two highest VB states at the Γ point of the $(AlAs)_4/(GaAs)_4$, $(AlAs)_4/(GaAs)_{12}$ and $(AlAs)_{12}/(GaAs)_4$ superlattices, respectively. (A) denotes localization in the AlAs layers and (B) denotes localization in the (GaAs) layers.

	$(AlAs)_4/(GaAs)_4$	$(AlAs)_4/(GaAs)_{12}$	$(AlAs)_{12}/(GaAs)_4$
CB1	2.31 (A)	2.21 (B)	2.28 (A)
VB1	0.41 (B)	0.51 (B)	0.39 (B)
VB2	0.38 (B)	0.48 (B)	0.31 (B)

Concerning the orbital character we note that for the CB states, if the localization appears in the AlAs slabs of the superlattice, then the main contribution is of p_z character, while if the localization is in the well layer or in the GaAs slabs of the superlattice then the main contribution is of s character. For the VB states, they have basically the heavy-hole and light-hole character, but the strict equality of p_x and p_y components is not satisfied.

4. Conclusions

We have studied the different states at the $\bar{\Gamma}$ point of embedded GaAs quantum wells in semi-infinite (AlAs)/(GaAs) superlattices by means of an ETB sp^3s^* model including spin–orbit splitting. We find that there are bound states in the well region for different combinations of the well thickness and the superlattice period. We find localized states in the embedded-well region for thicknesses which depend on the superlattice periods. These thicknesses are also different for the CB and VB states for a given superlattice. In the cases analysed here the CB states appear when $n \geqslant 8$, n being the number of GaAs layers in the embedded well, as in the normal quantum well. For the VB states we obtain bound states for some thicknesses only, as opposed to the normal quantum well case, in which there were

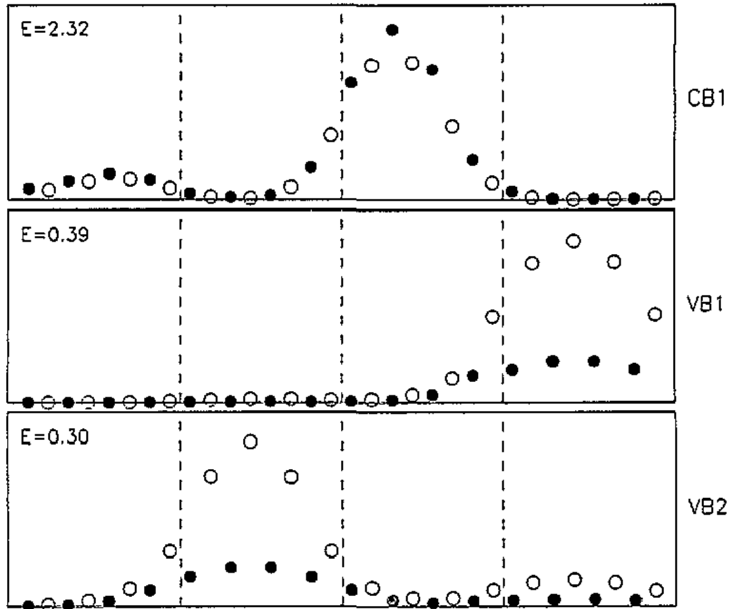

Figure 1. Distribution of the spectral strength in the different layers of an embedded GaAs slab of 4 layers, between a semi-infinite AlAs substrate (left) and a semi-infinite $(AlAs)_4/(GaAs)_4$ superlattice (right), where the first slab, starting from the left, corresponds to the AlAs and the second one corresponds to the GaAs. (a) CB1 state; (b) VB1 state; (c) VB2 state. (•, cations; ○, anions).

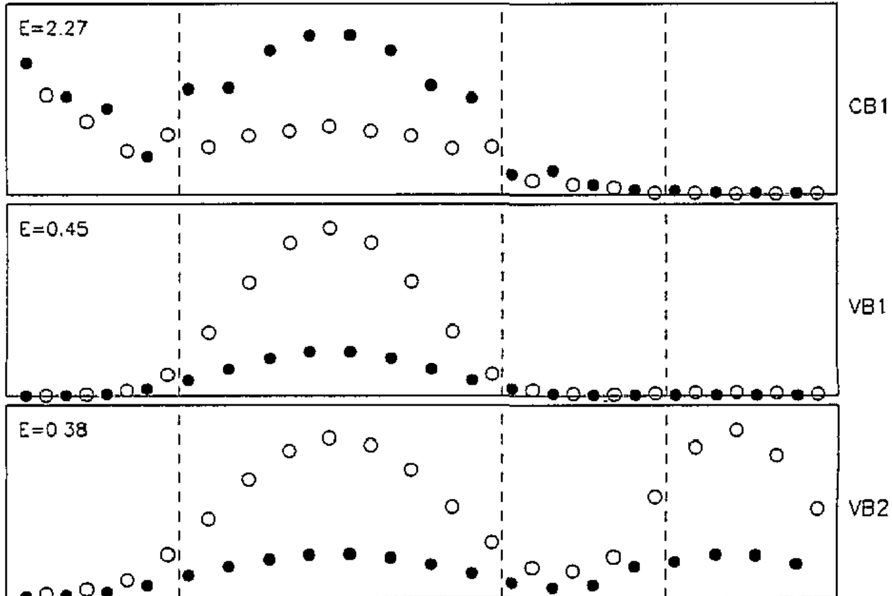

Figure 2. As in figure 1 for an embedded GaAs slab of 8 layers.

always bound states for any quantum well thickness, by using the same theoretical model. For energies quite close to those of the corresponding states in the infinite superlattices, and

if the thickness of the embedded layer is quite close to that of the GaAs layer in the infinite superlattice, we find localization in the embedded well and in the superlattice. This picture is more general than that emerging from the experimental data available, but agrees with the existing experimental information. In [4] the authors used a terminating quantum well with a width twice that of the wells in the superlattice to form a low energy, localized Tamm-like state. Our results for the $(AlAs)_{12}/(GaAs)_4$ and $(AlAs)_4/(GaAs)_4$ superlattices indicate that we have clear low energy, localized states in the embedded well (Tamm-like states) when its width is equal to or larger than twice the width of the wells in the superlattice. For smaller thicknesses of the embedded well we can have states which show localization only in the superlattice or which have spectral strength both in the embedded well and in the superlattice layers. The CB states localized in the well region exhibit s orbital character while those in the VB energy range can be broadly classified according to the usual scheme of heavy and light holes. The use of the ETB Hamiltonian guarantees the inclusion of band mixing and allows for a more realistic study than those performed until now with the Kronig–Penney model.

Acknowledgments

We are grateful to Professor F García-Moliner for helpful discussions and the critical reading of the manuscript. This work was partially supported by the Consejo Nacional de Ciencia y Tecnología (México) under grant No 2067E9302, the Dirección General de Investigación Científica y Técnica (Spain) under grant No PB93-1251 and the European Community under contract No CI1*-CT94-0046.

References

[1] Ohno H, Méndez E E, Brum J A, Hong J M, Agulló-Rueda F, Chang L L and Esaki L 1990 *Phys. Rev. Lett.* **64** 2555
[2] Ohno H, Méndez E E, Alexandrou A and Hong J M 1992 *Surf. Sci.* **267** 161
[3] Yeganek M S, Qi J, Yodh A G and Tamargo M C 1992 *Phys. Rev. Lett.* **68** 3761
[4] Agulló-Rueda F, Méndez E E, Ohno H and Hong J M 1990 *Phys. Rev.* B **42** 1470
[5] Bradshaw J L, Leavitt R P, Pham J T and Towner F J 1994 *Phys. Rev.* B **49** 1882
[6] Kucharczyk R and Stęślicka M 1992 *Solid State Commun.* **81** 557; 1992 *Solid State Commun.* **84** 727
[7] Huang F J 1990 *Appl. Phys. Lett.* **57** 1669, 2199
[8] Stęślicka M, Kucharczyk R and Glasser M L 1990 *Phys. Rev.* B **42** 1458
[9] Bloss W L 1991 *Phys. Rev.* B **44** 8035
[10] Jaskólski W 1992 *Phys. Rev.* B **45** 4398
[11] Masri P, Dobrzynski L, Djafari-Rouhani B and Idiodi J O A 1986 *Surf. Sci.* **166** 301
[12] Zhang J and Ulloa S E 1988 *Phys. Rev.* B **38** 2063
[13] Zhang J, Ulloa S E and Schaich W S 1991 *Phys. Rev.* B **43** 9865
[14] García-Moliner F and Velasco V R 1992 *Theory of Single and Multiple Interfaces* (Singapore: World Scientific)
[15] Arriaga J, García-Moliner F and Velasco V R 1993 *Prog. Surf. Sci.* **42** 271
[16] Arriaga J, García-Moliner F and Velasco V R 1993 *J. Phys.: Condens. Matter* **5** 5429
[17] Vogl P, Hjalmarson H P and Dow J D 1983 *J. Phys. Chem. Solids* **44** 365
[18] Chadi D J 1977 *Phys. Rev.* B **16** 790
[19] Muñoz M C, Velasco V R and García-Moliner F 1989 *Phys. Rev.* B **39** 1786
[20] García-Moliner F and Velasco V R 1991 *Phys. Rep.* **200** 83
[21] Contreras-Solorio D A, Velasco V R and García-Moliner F 1993 *Phys. Rev.* B **48** 12 319
[22] Haussy B, Priester C, Allan G and Lannoo M 1987 *Phys. Rev.* B **36** 1105
[23] Flores F, Durán J C and Muñoz A 1987 *Phys. Scr.* T **19** 102
[24] Muñoz A, Sánchez-Dehesa J and Flores F 1987 *Europhys. Lett.* **2** 385
[25] Muñoz A, Sánchez-Dehesa J and Flores F 1987 *Phys. Rev.* B **35** 6468

[26] Platero G, Sánchez-Dehesa J, Tejedor C and Flores F 1986 *Surf. Sci.* **168** 553

[27] Armelles G, Castrillo P, Dominguez P S, González L, Ruiz A, Contreras D A, Velasco V R and García-Moliner F 1993 *J. Physique Coll.* **3** C5 283

[28] Armelles G, Castrillo P, Dominguez P S, González L, Ruiz A, Contreras-Solorio D A, Velasco V R and García-Moliner F 1994 *Phys. Rev.* B **49** 14 020

[29] Vlaev S, Velasco V R and García-Moliner F 1994 *Phys. Rev.* B **50** 4577

[30] Vlaev S, Velasco V R and García-Moliner F 1995 *Phys. Rev.* B at press

[31] Jouanin C, Hallaoui A and Bertho D 1994 *Phys. Rev.* B **50** 1645

[32] Grosso G, Moroni S and Pastori Parravicini G 1989 *Phys. Rev.* B **40** 12 328

[33] Arriaga J, Armelles G, Muñoz M C, Rodriguez J M, Castrillo P, Recio M, Velasco V R, Briones F and García-Moliner F 1991 *Phys. Rev.* B **43** 2050